obtained from Eqs. (36–38) and (39–41) with the aid of Eqs. (44) and (45).

References

[1] Bruun, E. R., "Thermal Deflection of a Circular Sandwich Plate," *AIAA Journal*, Vol. 1, No. 5, May 1963, pp. 1213–1215.

[2] Huang, J. C. and Ebcioglu, I. K., "Circular Sandwich Plate under Radial Compression and Thermal Gradient," *AIAA Journal*, Vol. 3, No. 6, June 1965, pp. 1146–1148.

[3] Kao, J. S., "Bending of Circular Sandwich Plates," *Journal of the Engineering Mechanics Division*, ASCE, Vol. 91, No. EM4, Proc. Paper 4449, Aug. 1965, pp. 165–176.

[4] Ebcioglu, I. K., "Thermoelastic Equations for a Sandwich Panel under Arbitrary Temperature Distribution, Transverse Load, and Edge Compression," *Proceedings of the 4th U.S. National Congress of Applied Mechanics*, 1962, pp. 537–546.

[5] Forray, M. and Newman, M., "Bending of Circular Plates due to Asymmetric Temperature Distribution," *Journal of the Aerospace Sciences*, Vol. 28, No. 10, Oct. 1961, pp. 773–778.

Heat Transfer and Pressure on a Hypersonic Blunt Cone with Mass Addition

C. C. Pappas* and George Lee*

NASA Ames Research Center, Moffett Field, Calif.

Nomenclature

B = dimensionless transpiration parameter, $B = \dot{m}\Delta H/q_0$
ΔH = enthalpy potential
$\dot{m}$ = mass flow of transpiration gas per unit area
p = pressure on model surface
q = heat flux to model surface
q_0 = heat flux to surface at zero transpiration
R = nose radius of model
S = surface distance along model measured from stagnation point
U_∞ = freestream velocity
ρ_∞ = freestream density

Introduction

THE thermal protection of a hypersonic vehicle is often accomplished by ablation or transpiration cooling techniques. Secondary effects, such as changes in surface pressure, can accompany the ablation or transpiration. In any case, it is known that the molecular weight of the ablated or transpired gases can strongly influence the heat transfer and pressure on the vehicle. Information, in general, both experimental and theoretical, concerning this problem is quite meager. Therefore, an experimental program was undertaken (and a theoretical program instituted) to study this problem. The theory has been described in Ref. 1. In the experimental program, the effect of molecular weight of the injected gases helium, air, argon, and freons (with molecular weight variation of 4–200) on the heat transfer and pressure on a blunt cone was studied by the transpiration technique. All gases were injected with an approximate uniform distribution along the model. A portion of the experimental work, together with some comparisons of the theories with typical data, will be described herein.

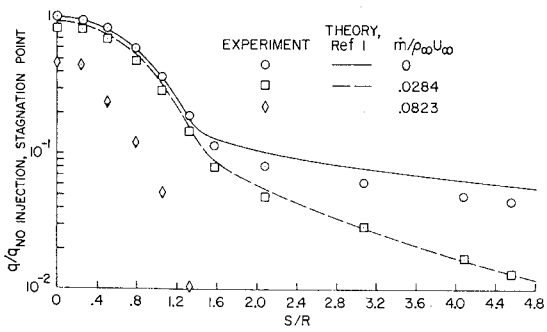

Fig. 1 Heat transfer with uniform argon injection.

Experimental Procedures

All of the tests that are reported here were conducted in a hypersonic air stream at a nominal Mach number of 13.4, total stream enthalpy near 2100 Btu/lb, and Reynolds number of 31,000 per ft. Mass flow rate of the injected gases varied from zero to over 50% of the freestream mass flow. In all cases, the higher injected gas flow rates were sufficient to reduce stagnation point heat transfer to zero.

The test models were hemispherically blunted cones consisting of a 1-in. nose radius with a 3.5-in.-long, 7.5° semivertex angle conical afterbody. They were made of 34% porous sintered nickel with a wall thickness of 0.1 in. Thermocouples were spot welded on both inside and outside surfaces along two opposite rays of the heat-transfer model. Pressure orifices of up to 0.2 in. diam were located alternately along two rays of the pressure model. Locations of thermocouples and pressure orifices are indicated in the subsequent data presentation.

The cone wall thickness and porosity were selected to insure uniform surface mass addition over the whole model for the various external pressure distributions encountered during the tests. Local and over-all transpiration rates were measured for the models. The variation of the local mass flow rate measured over an 0.08 sq. in. area was within ±10% of the average value.

Heat transfer to the cone surface was obtained by measuring the time-temperature history of the porous wall immediately after the model was exposed to the high-speed air stream. All pertinent model temperature measurements were recorded during the 2-sec exposure time. Steady surface pressures were measured at the pressure transducers within approximately 1 sec after the model was exposed to the tunnel air stream.

Results and Discussion

An extensive amount of surface heat-transfer and pressure data on porous cones with surface mass addition of helium, air, argon, freon 22, freon 12, and freon C-318 was obtained in the experimental program. In Ref. 1, theory was used to calculate both surface heat transfer and pressure for the same test bodies but for a limited set of test conditions with argon and helium mass addition. Since an effort of this limited re-

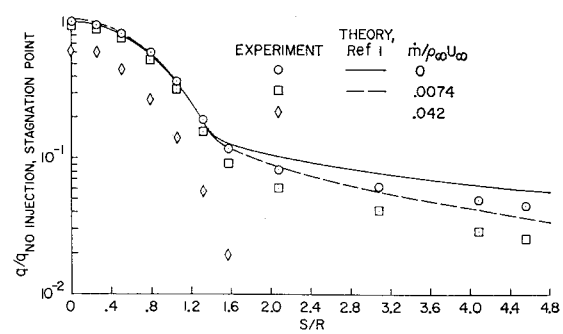

Fig. 2 Heat transfer with uniform helium injection.

Presented as Paper 69-716 at the AIAA Fluid and Plasma Dynamics Conference, San Francisco, Calif., June 16–18, 1969; submitted June 26, 1969; revision received February 27, 1970.

* Research Scientist.

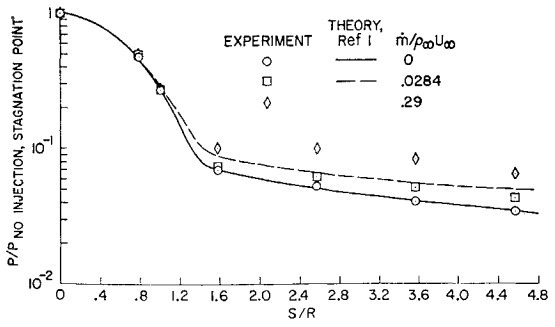

Fig. 3 Pressure distribution with uniform argon injection.

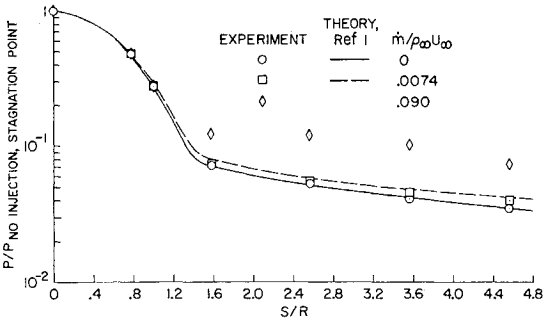

Fig. 4 Pressure distribution with uniform helium injection.

port is to assess theory the presentation of results is sometimes restricted to test conditions where theoretical comparisons are available. The stagnation point heat-transfer theory with mass addition of Ref. 2 is not restricted to the kind of gas added at the surface, and comparison of heat transfer is made for all the injection gases used in the tests.

Heat-transfer and pressure distribution

The effect of uniform argon injection on the surface heat transfer is presented in Fig. 1. Three typical heating rate distributions are shown for the specified mass addition rates. As expected, mass injection reduced the heating rate along the entire surface of the blunt cone. The percentage reduction in heat transfer, however, is more pronounced on the afterbody than on the nose of the model. As an example, for the case of the highest mass injection rate shown, the heating rate on the afterbody was reduced to zero, whereas it was reduced only in half at the stagnation point.

Theoretical calculations of the heat-transfer and pressure distributions on the blunt cone for a binary component boundary layer have been performed for the same test conditions, see Ref. 1. The theory is based on a combined inviscid blunt body and nonsimilar boundary-layer program. An important feature of this program is that iterations between the inviscid and boundary-layer solutions are considered, with the boundary-layer displacement thickness as the iteration variable.† The necessity of using the combined iterative solution for the heat transfer with and without argon injection is clearly shown in Ref. 1. Two of the final iterated solutions, one without injection and one with argon injection are included on Fig. 1. For zero mass injection, the predictions are higher than the data by approximately 20% on the afterbody, but are quite good on the nose. For the mass injection case, the agreement of theory with data is excellent over the whole body.

The experimental heat-transfer measurements for helium injection are presented and compared with theory in Fig. 2. The measurements and theory for zero injection are from the previous figure and are included for reference purposes. Although the general trends of the experimental measurements are predicted, specific differences are evident. For the mass injection case, the theory predicts about 5% rise in heat transfer over the non-injection case at the stagnation point, whereas experiment shows a near 5% decrease in heat transfer. Generally, for the helium injection comparison, the theory overpredicts the heat transfer all along the body by nearly 10% at the stagnation point and about 40% on the afterbody.

Since the theoretical solutions of the boundary layer and pressure distribution are iterative through the displacement thickness an examination of the predicted and experimental surface pressure distribution is now in order. Typical pressure distributions over the model without and with mass injection of argon are shown in Fig. 3. Near the stagnation region, and including nearly all of the hemispherical portion of the nose, the pressure was not affected by mass injection. On the afterbody, the pressure was strongly affected by mass injection. Increases in pressure of over a factor of 3 were measured at higher injection rates; see, for example, the last figure of this report. The higher pressures are caused by an increasing boundary-layer displacement thickness which, in turn, increases with increasing mass injection rate. The final iteration pressure distributions calculated in Ref. 1 are compared with measurement in Fig. 3, and good agreement is obtained over the entire model for zero injection and the specified blowing rate of argon. The zero iteration value of the pressure distribution for zero injection was about 10% below the final iteration solution for the afterbody. Substantial variations in afterbody pressures were noted with gas injection for the initial iteration solutions as compared to the final solution, see Ref. 1.

The pressure distribution over the body was also calculated for a case with helium injection. Agreement of theory with experiment is good, as shown in Fig. 4. Again, the necessity for iterating on the inviscid pressure and boundary-layer solutions is evident from an examination of Ref. 1.

The effect of molecular weight of the injected gases on the heat transfer to the stagnation point is shown in Fig. 5. In general, except for the freon gases, the effect of lowering molecular weight was to decrease the heat transfer. For the freon gases, the measurements at the stagnation point show no change in heat transfer with change in molecular weight from 86.5 to 200. Chemical reactions of the freon gases within the boundary layer may account for the lack of effect of molecular weight on the heat transfer. The theory of Yoshikawa, Ref. 2, for stagnation point heat transfer, which for the three lighter gases predicted the effect of molecular weight in Fig. 5 quite well, shows a continued small dependence of the heat transfer on the molecular weight of the freon gases. This theory, however, does not account for any chemical reactions occurring within the stagnation region, but does

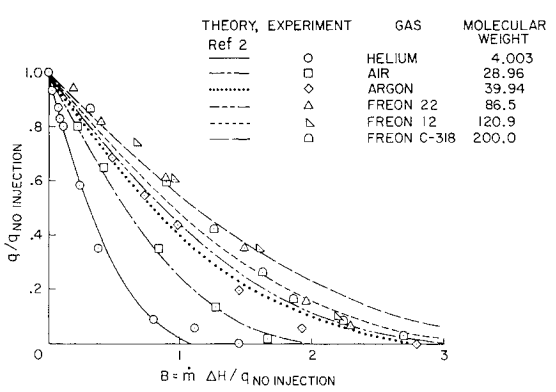

Fig. 5 Effect of injection gas on stagnation point heat transfer.

† Transverse curvature effects are also included in the injection and no-injection calculations.

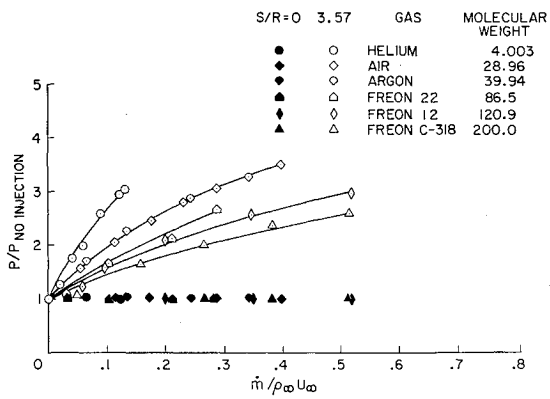

Fig. 6 Effect of injection gas on pressure distribution.

consider the effects of freestream density and nose radius in its formulation; therefore, the low-density flow of the present tests can be adequately represented by the theory.

The relative reduction in heat transfer measured on the afterbody due to injection of the various gases is similar to that in Fig. 5. The freon gases show the same heat reduction effectiveness.

The effect of the molecular weight of the injected gas on the surface pressure at the stagnation point and a representative point on the afterbody is shown in Fig. 6. At the stagnation point, molecular weight and rate of mass addition have no effect on the surface pressure. On the afterbody, molecular weight and injection rate have a very strong effect on surface pressure. Note that the freon gases have the expected individual effect of molecular weight on the increase in surface pressure as contrasted with the equal effect of the freons on the decrease in heat transfer with injection. The gases air and argon (mol. wt. 28.9 and 40.0, respectively) show an equivalent effect on the increase in surface pressure, whereas each gas had a distinct effect on the reduction in heat transfer. The inference is that the momentum thickness of the boundary layer for both air and argon injection has the same effective distribution along the body.

Concluding Remarks

Agreement between theory and experiment was good for the stagnation point heat transfer with helium, air, and argon injection. The three freon gases showed an equal effect on the reduction in heat transfer at the stagnation point; whereas theory showed a small molecular weight effect.

The prediction of the heat-transfer distribution was good over the whole cone for argon injection. Predictions of heat transfer on the forebody with and without helium injection were fairly good, and predictions on the afterbody were 40% high with helium injection and about 25% high without injection. The lack of agreement with helium injection reflects the disparity with no injection.

An inviscid surface pressure prediction, which had been coupled to a nonsimilar boundary-layer theory, was generally in good agreement with the measured surface pressure over the whole blunt cone model for helium and argon injection and for no injection.

References

[1] Lewis, C. H., Adams, J. C., and Gilley, G. E., "Effects of Mass Transfer and Chemical Non-equilibrium on Slender Blunted Cone Pressure and Heat Transfer Distribution at $M_\infty = 13.2$," AEDC TR-68-214, Nov. 1968, ARO Inc.

[2] Yoshikawa, K. K., "Linearized Theory of Stagnation Point Heat and Mass Transfer at Hypersonic Speeds," TN D-5246, 1969, NASA.

Influence of Gravity on the Performance of a Conical Vortex Separator

K. R. Burton*
Convair Division of General Dynamics, San Diego, Calif.

Introduction

Vortex separators are widely used for the separation of the phases of a two-phase fluid and consist essentially of a conical channel containing the swirling mixture. The heavy particles are thrown to the wall, where a boundary layer forms in the film of heavy fluid. Due to the potential motion of the bulk of the fluid, a pressure field develops which induces a secondary flow in the boundary layer. It is this phenomenon that causes the flow of heavy fluid toward the small open end of the cone and is responsible for the effectiveness of the vortex separator. A gravity force, depending upon its direction, can either increase or reduce the swirl-induced flow.

Lawler and Ostrach[1] discussed the effect of gravity on vortex separators and defined a Froude number for qualitative analysis of the relative strength of the gravitational and inertial forces. Their analytical results were obtained by considering the body force to act on the heavy fluid, both within and outside the boundary layer. Combining the pressure gradient and body force terms allowed use of Taylor's original solution[2] for boundary-layer motion in a swirling conical flow.

This note differs from Ref. 1 in that the effect of gravity is neglected in the thin region of heavy fluid outside the boundary layer. Such an assumption allows explicit prediction of the effect of a body force on the boundary-layer flow, and results in definition of the limiting condition for use of a vortex separator in an adverse gravity field.

Taylor's Swirl Problem

An incompressible fluid enters a conical tube tangentially at the large end. The conical chamber, whose apex angle is 2α, is so designed that the axial component of velocity is small compared to the swirl component. Except for a thin layer along the wall, the velocity is given by Ω/r, where r is the distance from the axis and Ω is the circulation.

The equations of motion with the usual boundary-layer approximations are listed below, in spherical coordinates, with the origin at the apex of the cone:

$$u\frac{\partial u}{\partial R} + \frac{v}{R}\frac{\partial u}{\partial \theta} - \frac{w^2}{R} = -\frac{1}{\rho}\frac{\partial p}{\partial R} + \frac{\nu}{R^2}\frac{\partial^2 u}{\partial \theta^2} \qquad (1)$$

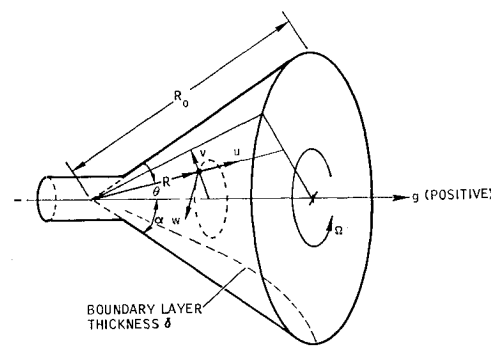

Fig. 1 Coordinate system.

Received August 11, 1969; revision received January 21, 1970. This work was performed under Contract NAS 1-8494, NASA Langley Research Center. The author wishes to acknowledge the helpful suggestions contributed by E. A. Evans.

* Senior Thermodynamics Engineer.